Supporting Information for

Selective Synthesis of Rhodium-based Nanoframe Catalysts by Chemical Etching of 3d Metals

Zhi-Ping Zhang, Wei Zhu, Chun-Hua Yan and Ya-Wen Zhang*

Beijing National Laboratory for Molecular Sciences, State Key Laboratory of Rare Earth Materials Chemistry and Applications, PKU-HKU Joint Laboratory in Rare Earth Materials and Bioinorganic Chemistry, College of Chemistry and Molecular Engineering, Peking University, Beijing 100871, China.

Experimental Section

Synthesis

Chemicals. Oleylamine (OAm, J&K), $RhCl_3 \cdot 3H_2O$ (A.R., Sinopharm Chemical Reagent Co. Ltd, China), $CuCl_2 \cdot 2H_2O$ (A.R., Beijing Hongxing Chemical Factory, China), $NiCl_2 \cdot 6H_2O$ (A.R., Beijing Yili Fine Chemical Reagent Corp., China), $PdCl_2$ (A.R., Shenyang Institute of Nonferrous Metal, China), HCl solution (A.R., Beijing Chemical Works, China), $NaBH_4$ (A.R., Tianjin Xuanang Trading Co. Ltd. of Science and Industry, China), carbon black (Vulcan XC-72), $N_2H_4 \cdot H_2O$ (98%, J&K), ethanol (A.R.), cyclohexane (A.R.) were used as received. The water used in all experiments was ultrapure.

Synthesis of Rh-Cu Nanooctahedrons. The precursors, 0.066 mmol of $RhCl_3 \cdot 3H_2O$ (s), 0.100 mmol of $CuCl_2 \cdot 2H_2O$ (s), and 12 mL of OAm were put in a 100 mL three-neck flask. And only one neck was equipped with a thermometer. Then the reaction container was heated to 180 ℃ upon stirring continually in air. During the heating-up process, the color of the reaction mixture turned from blue to green, then to yellow. In order to ensure that the solid $RhCl_3$ and $CuCl_2$ could be completely dissolved into the oleylamine, the reaction mixture was held at 180 ℃ for 60 min with stirring. After 60min, the brown reaction mixture was transferred into a 25 mL Teflon-lined stainless steel autoclave, which had been preheated to 70 ℃, to reduce the effect of oxygen inside the Teflon bottle on the reducing capability of OAm. The autoclave was then heated at 180 ℃ for 24 h before it was cooled to room temperature. The mixture was centrifuged at 9600 rpm for 12 min with importing 20 mL of ethanol, followed by washing with some cyclohexane/ethanol. Finally, the precipitated Rh-Cu nanoparticles were redispersed in cyclohexane.

If 0.066 mmol of $RhCl_3 \cdot 3H_2O$ (s), 0.100 mmol of $CuCl_2 \cdot 2H_2O$ (s), and 12 mL of OAm was kept in the three-neck flask at 180 ℃ for 24 h, no nanoparticles were produced because the metal precursors could not be reduced by OAm in air.

Synthesis of Rh-Cu Nanooctahedrons/C. Rh-Cu nanooctahedrons (0.019 mmol of Rh) and 12.5 mg of carbon black was ultrasonically dispersed in a mix of 15 mL of cyclohexane and 5 mL of acetone for 2 h. The mixture was centrifuged at 9000 rpm for 10 min, and washed with cyclohexane for two times. The precipitate was

dispersed with 17 mL of acetic acid, then transferred to a 25 mL Teflon-lined stainless steel autoclave, and heated at 70 ℃ for 12 h. The mixture was centrifuged at 9000 rpm for 10 min with importing 20 mL of ethanol, then washed with ethanol for three times. Finally, the precipitated Rh-Cu nanooctahedrons/C (the loaded content of Rh was 14.6 wt%) were dried under vacuum or redispersed in 8 mL of ethanol.

Synthesis of Rh-Cu Nanooctahedral frames/C. Rh-Cu nanooctahedrons/C (0.007 mmol of Rh) was dispersed in 5 mL of H_2O, then mixed with 7.5 mL of dilute HCl solution (0.80 mol/L). The mixture was heated to 80 ℃ in air, and kept for 9 h. Finally, the precipitated Rh-Cu nanooctahedral frames/C (the loaded content of Rh was 9.3 wt%) were centrifuged and washed with ethanol for three times, then dried under vacuum.

Synthesis of Rh-Pd-Cu Nanopolyhedrons. The synthesis of Rh-Pd-Cu nanopolyhedrons was the same as that of Rh-Cu nanooctahedrons except that the precursors were 0.066 mmol of $RhCl_3·3H_2O$ (s), 0.025 mmol of $PdCl_2$ (s), 0.175 mmol of $CuCl_2·2H_2O$ (s) and 14 mL of OAm.

Synthesis of Rh-Pd-Cu Nanopolyhedrons/C. The synthesis of Rh-Pd-Cu nanopolyhedrons/C was the same as that of Rh-Cu nanooctahedrons/C except using Rh-Pd-Cu nanopolyhedrons (0.021 mmol of Rh) rather than Rh-Cu nanooctahedrons (0.019 mmol of Rh).

Synthesis of Rh-Pd-Cu Nanopolyhedral Frames/C. The synthesis of Rh-Pd-Cu nanopolyhedral frames/C was similar to that of Rh-Cu nanooctahedral frames/C. Rh-Pd-Cu nanopolyhedrons/C (0.009 mmol of Rh) were dispersed in 5 mL of H_2O, then mixed with 7.5 mL of dilute HCl solution (0.80 mol/L). The mixture was heated to 60 ℃ in air, and kept for 25 min.

Synthesis of Rh-Ni Nanopolyhedrons. The synthesis of Rh-Ni nanopolyhedrons was the same as that of Rh-Cu nanooctahedrons except that the precursors were 0.023 mmol of $RhCl_3·3H_2O$ (s) and 0.080 mmol of $NiCl_2·6H_2O$ (s), and the solvothermal temperature was lifted to 210 ℃.

Synthesis of Rh-Ni Nanopolyhedrons/C. The synthesis of Rh-Ni nanopolyhedrons/C was the same as that of Rh-Cu nanooctahedrons/C except using Rh-Ni nanopolyhedrons (0.015 mmol of Rh) rather than Rh-Cu nanooctahedrons (0.019 mmol of Rh).

Synthesis of Rh-Ni Porous Nanoparticles/C. The synthesis of Rh-Ni porous nanoparticles/C was similar to that of Rh-Cu nanooctahedral frames/C. Rh-Ni nanopolyhedrons/C (0.005 mmol of Rh) were dispersed in 5 mL of H_2O, then mixed with 5.3 mL of dilute HCl solution (0.68 mol/L). The mixture was heated to 80 ℃ in air, and kept for 6 h.

Synthesis of Rh/C. The synthesis of Rh/C was followed by a modified process as described in Ref. S1. 0.078 mmol of $RhCl_3$ was ultrasonically dissolved in 2 mL of H_2O, then 40 mg of carbon black was added to the aqueous solution with sonication and stirring for 5 min. Then, 2 mL of solution $NaBH_4$ (0.075 M) was rapidly added to the mixture, followed by stirring for 1 h. Finally, the precipitated Rh/C (the loaded content of Rh was 9.4 wt%) was centrifuged and washed with ethanol for three times, then dried under vacuum.

Synthesis of Cu/C. The synthesis of Cu/C was followed by a modified process as described in Ref. S1. 0.100 mmol of $CuCl_2$ was ultrasonic dissolved in 2.5 mL of H_2O, then 30 mg of carbon black was added to the aqueous solution with sonication and stirring for 5 min. Then 1.5 mL of $NaBH_4$ solution (0.352 M) was rapidly added to the mixture, followed by stirring for 1h. Finally, the precipitated Cu/C (the loaded content of Cu was 15.1 wt%) was centrifuged and washed with ethanol for three times, then dried under vacuum.

Synthesis of $Rh_{1.7}Cu/C$. The synthesis of $Rh_{1.7}Cu/C$ was followed by a modified process as described in Refs. S1 and S2. The synthesis of Rh-Cu/C was the same as that of Cu/C except that the precursors were 0.096 mmol of $RhCl_3$ and 0.050 mmol of $CuCl_2$. Finally, the precipitated $Rh_{1.7}Cu/C$ (the loaded content of Rh was 13.3 wt%) was centrifuged and washed with ethanol for three times, then dried under vacuum.

Catalytic Reactions for Hydrous Hydrazine Decomposition.

Catalytic reactions were carried out by following the method previously reported by Xu and coworkers with some modifications (see Ref. S1). Typically, Rh-based NP catalysts (0.01 mmol Rh) and 1 mL of ultrapure water were stirred in the glass reaction tube. The reaction temperature was kept constant at 25 ℃ using a water bath. 1.0 mmol of hydrazine monohydrate was injected to the reaction tube to initiate hydrazine decomposition reaction. The gas released during the reaction was passed through a hydrochloric acid solution (1.0 M) to absorb NH_3, and measured using a self-made gas burette. For the catalytic reactions using carbon black or Cu/C, the amount of catalysts is 20 mg or 0.01 mmol of Cu, respectively.

Calculation of turnover frequency (TOF) and the H_2 selectivity.

The hydrazine decomposition mainly includes two reactions: complete decomposition, $H_2NNH_2 \rightarrow N_2 (g) + 2H_2(g)$ (reaction 1); and incomplete decomposition, $3H_2NNH_2 \rightarrow 4NH_3(g) + N_2(g)$ (reaction 2). TOFs are calculated on the basis of the data at 50% completion of hydrazine decomposition, measured in $[mol\ H_2][mol\ Rh]^{-1}h^{-1}$ (Rh = 0.01 mmol). And given that χ represents the selectivity toward H_2 generation, so the combined reaction for reaction (1) and (2) can be expressed as $3H_2NNH_2 \rightarrow 4(1-\chi)NH_3(g) + (1+2\chi)N_2(g) + 6\chi H_2(g)$ (reaction 3), and H_2 selectivity can be expressed as $\chi = (3\lambda-1)/8\ [\lambda = n(H_2+N_2)/n(H_2NNH_2)]$ (Ref. S3), and the value of $n(H_2NNH_2)$ in this work is 1.0 mmol.

Instrumentation.

Samples for transmission electron microscopy (TEM) observations were prepared by drying few droplets of cyclohexane dispersion of Rh-Cu nanooctahedrons or few droplets of ethanol dispersion of Rh-Cu nanooctahedrons/C or Rh-Cu nanooctahedral frames/C on nickel grids coated with amorphous carbon membranes. For Rh-Pd-Cu systems, they were similar to those of Rh-Cu systems. For Rh-Ni systems, they were similar to those of Rh-Cu systems except using copper grids rather than nickel grids. TEM, selected area electron diffraction (SAED), high-resolution TEM (HRTEM), and energy dispersive X-ray spectroscopy (EDS) analyses were

performed on a FEG-TEM (JEM-2100F, JEOL, Japan) operated at 200 kV. X-ray diffraction (XRD) patterns were obtained on a D/MAX-2000 diffractometer (Rigaku, Japan) with Cu-Kα radiation. Inductively coupled plasma-atomic spectroscopy (ICP-AES) analysis was performed on a Profile Spec ICP-AES spectrometer (Leeman, USA). X-ray photoelectron spectroscopy (XPS) analysis was taken on an Axi Ultra imaging photoelectron spectronmeter (Kratos, UK).
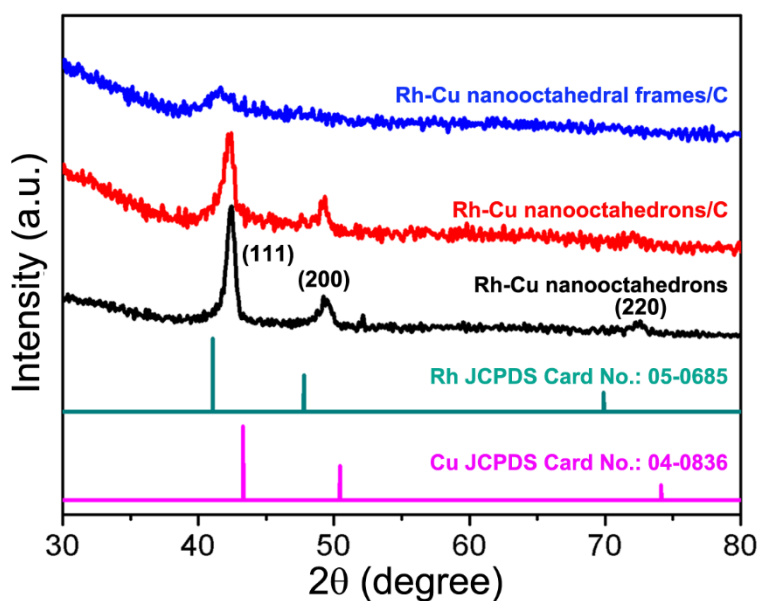

Figure S1. XRD patterns of as-prepared Rh-Cu nanooctahedrons, Rh-Cu nanooctahedrons/C (the loaded content of Rh was 14.6 wt%) and Rh-Cu nanooctahedral frames/C (the loaded content of Rh was 9.3 wt%), with the standard data for *fcc* Rh (JCPDS Card No.: 05-0685) and *fcc* Cu (JCPDS Card No.: 04-0836) as references.
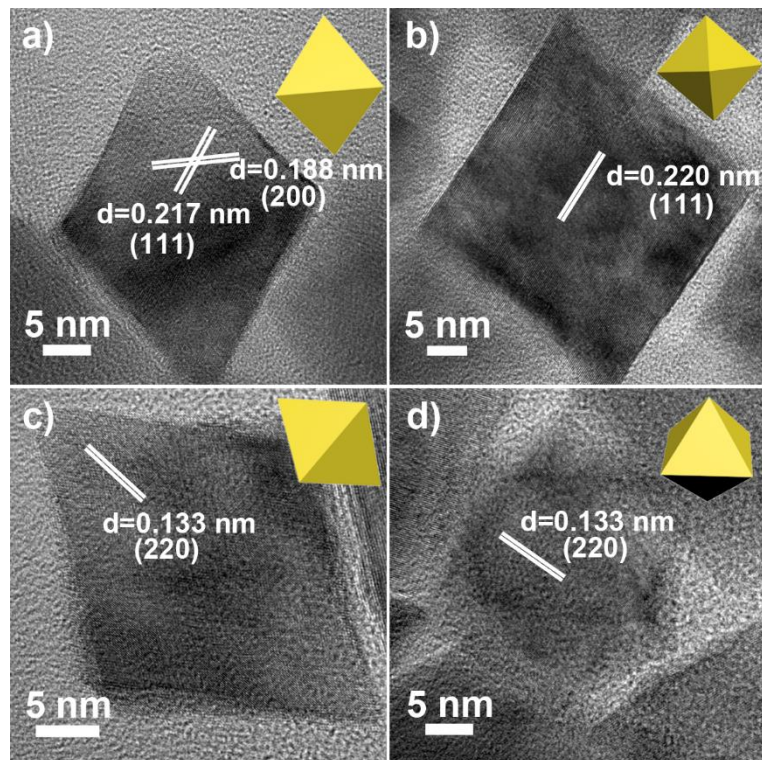
Figure S2. HRTEM images of Rh-Cu nanooctahedrons orientated along different directions.
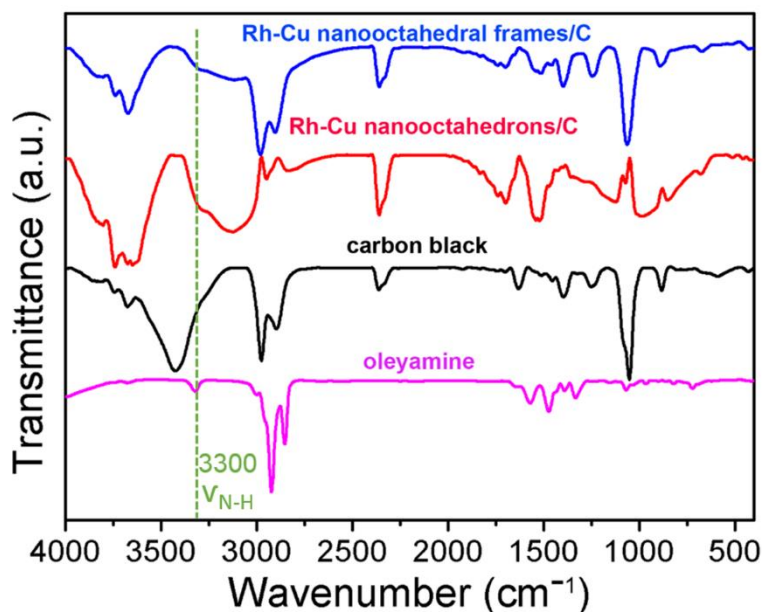
Figure S3. FTIR spectra of oleyamine, carbon black, Rh-Cu nanooctahedrons/C, and Rh-Cu nanooctahedral frames/C. The very weak absorption peak at 3300 cm^{-1} due to the N-H stretching mode (Ref. S4) indicated most of OAm was removed from the surfaces of Rh-Cu nanooctahedrons/C and Rh-Cu nanooctahedral frames/C.
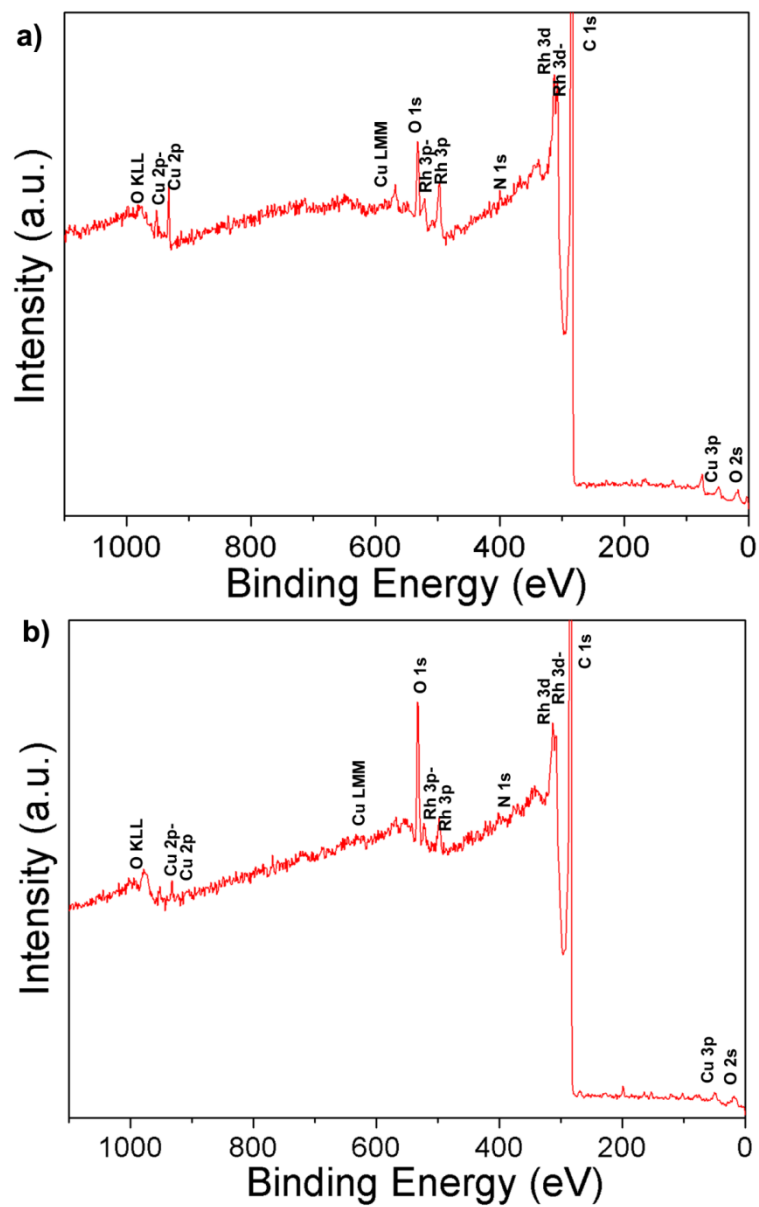
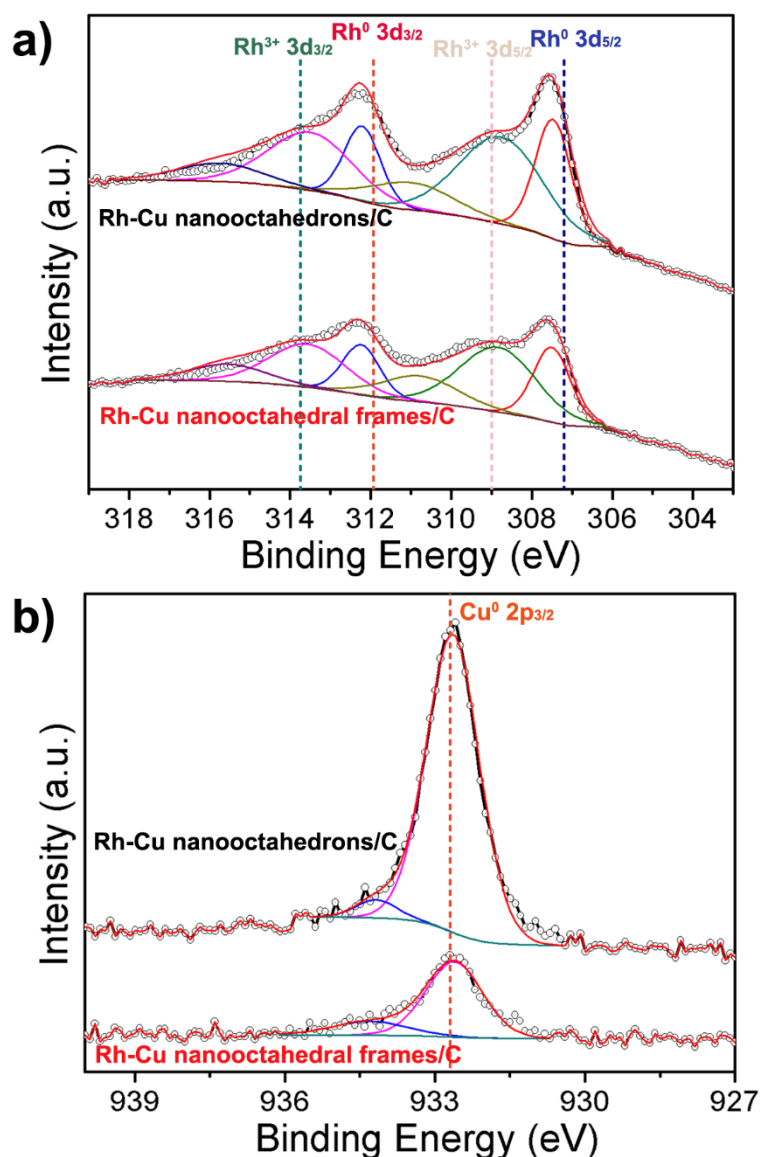**Figure S4.** XPS full spectra of (a) Rh-Cu nanooctahedrons/C and (b) Rh-Cu nanooctahedral frames/C.

Figure S5. (a) Rh 3d and (b) Cu $2p_{3/2}$ XPS spectra of Rh-Cu nanooctahedrons/C and Rh-Cu nanooctahedral frames/C. For Rh-Cu nanooctahedrons/C, through the calculation by dividing the sum of corrected area of the peak ascribed to Rh^0 $3d_{3/2}$ (311.9 eV, see Ref. S5) and that of Rh^0 $3d_{5/2}$ (307.2 eV, see Ref. S5) by the total corrected area of Rh 3d (Ref. S5), it was noted that a high proportion of surface Rh was in oxidized state. On the other hand, through the calculation of dividing the corrected area of the peak ascribed to Cu^0 $2p_{3/2}$ (932.7 eV, see Ref. S5) by the total corrected area of the Cu $2p_{3/2}$ peak, it was known that most of Cu element was in its metallic state after HAc treatment. However, for Rh-Cu nanooctahedral frames/C, more Rh and a small fraction of Cu were in oxidized states after HCl etching.
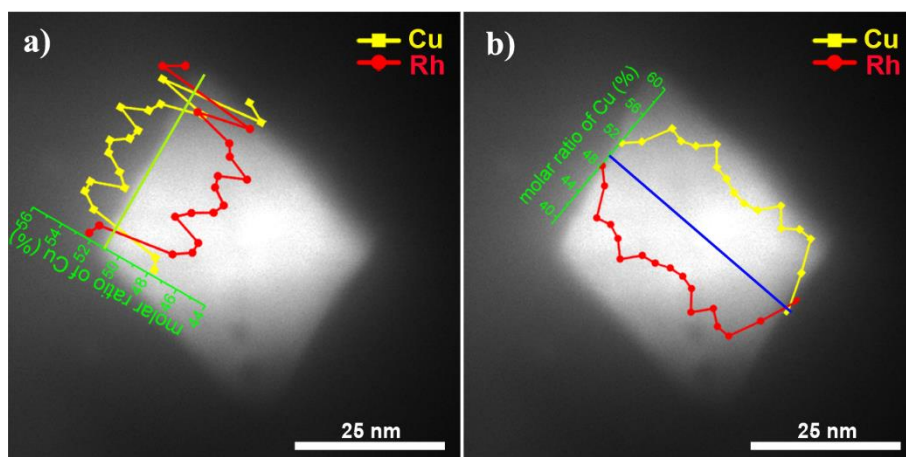
Figure S6. EDS line scan profiles of Rh-Cu nanooctahedrons/C. The average molar ratios of Rh in (a) and (b) are 49% and 44%, respectively.
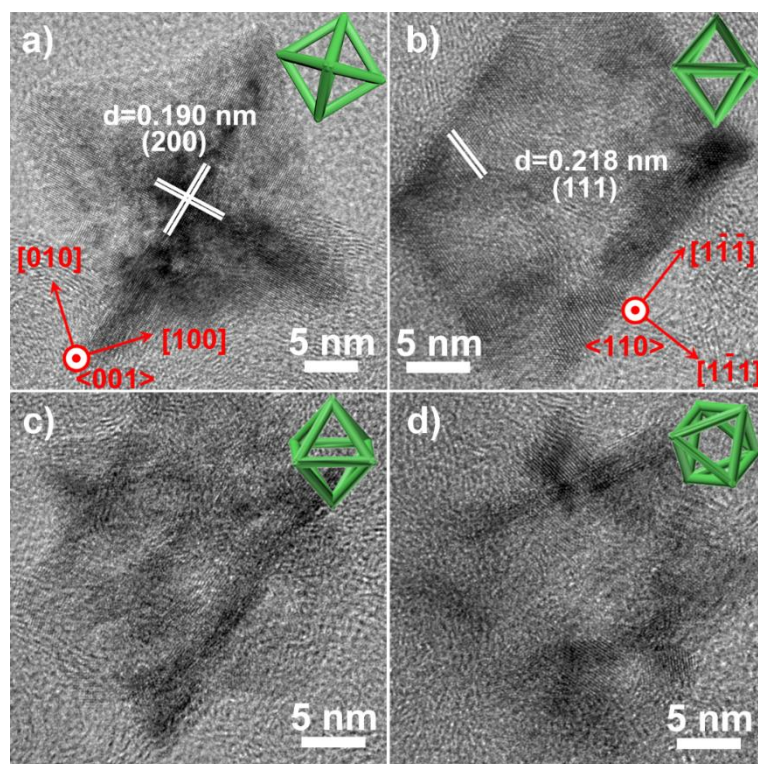
Figure S7. HRTEM images of Rh-Cu nanooctahedral frames/C orientated along different directions.
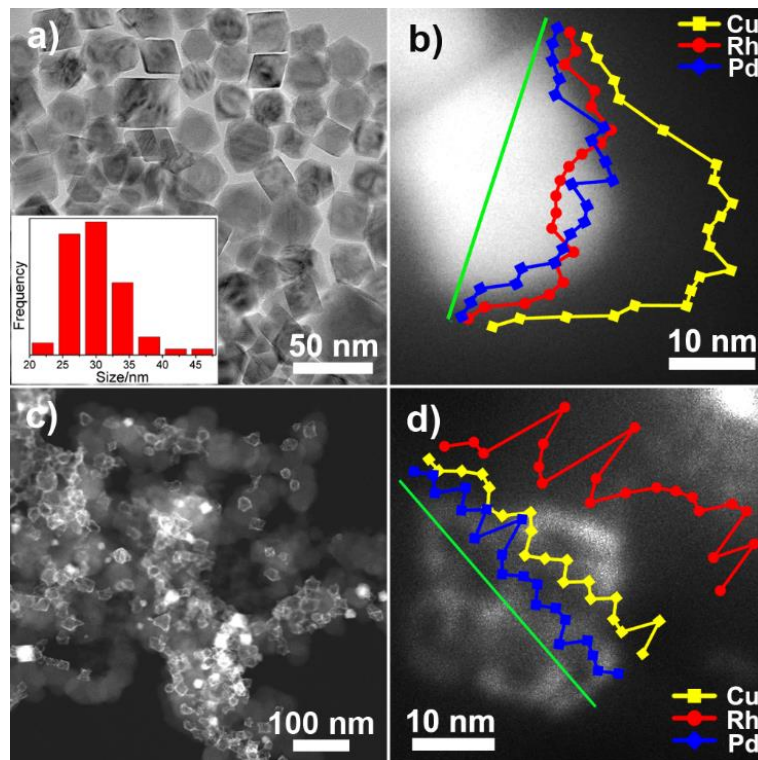
Figure S8. TEM image (a) and EDS line scan profiles (b) of Rh-Pd-Cu nanopolyhedrons. HAADF-STEM image (c) and EDS line scan profiles (d) of Rh-Pd-Cu nanopolyhedral frames/C. Inset in panel (a) is the size distribution histogram of Rh-Pd-Cu nanopolyhedrons.
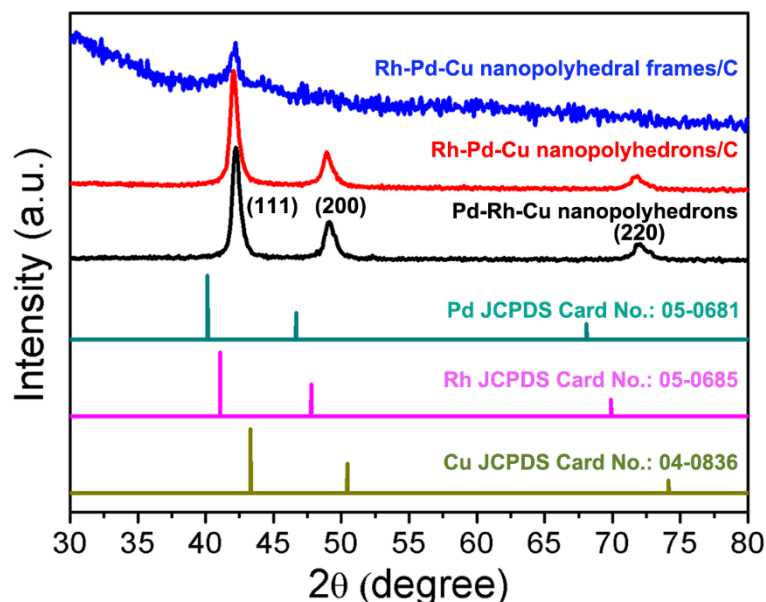

Figure S9. XRD patterns of as-prepared Rh-Pd-Cu nanopolyhedrons, Rh-Pd-Cu nanopolyhedrons/C and Rh-Pd-Cu nanopolyhedral frames/C, with the standard data for *fcc* Pd (JCPDS Card No.: 05-0681), *fcc* Rh (JCPDS Card No.: 05-0685) and *fcc* Cu (JCPDS Card No.: 04-0836) as references.
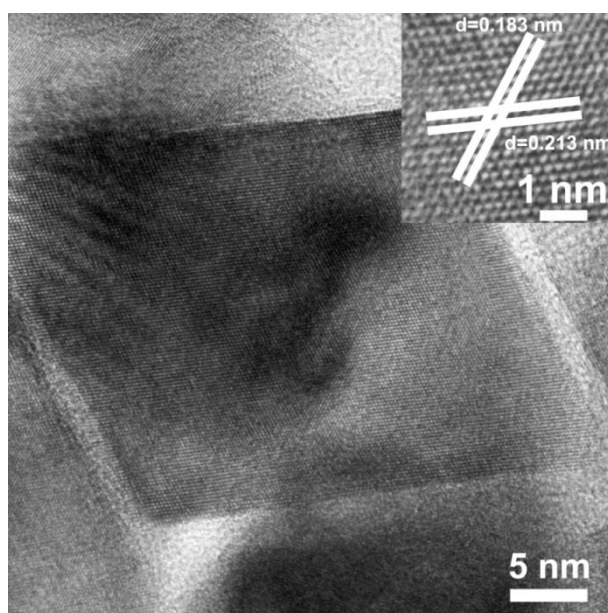
Figure S10. HRTEM image of Rh-Pd-Cu nanopolyhedrons.
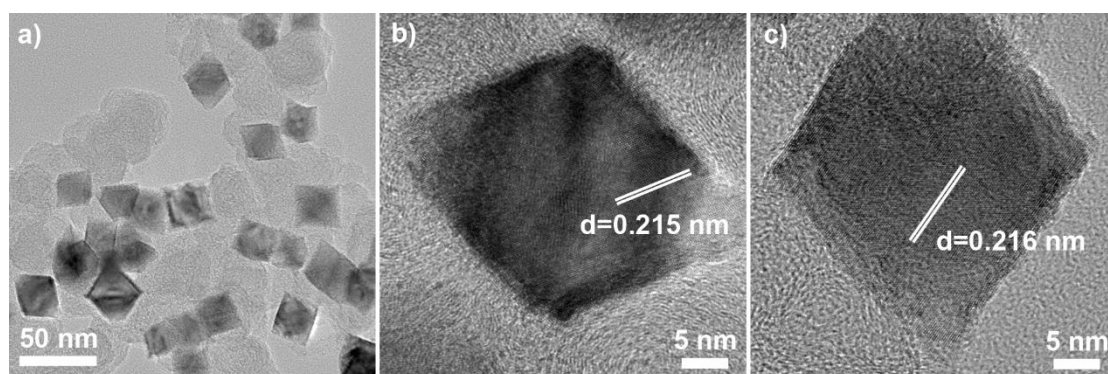
Figure S11. (a) TEM image, (b) and (c) HRTEM images of Rh-Pd-Cu nanopolyhedrons/C after treated in acetic acid.
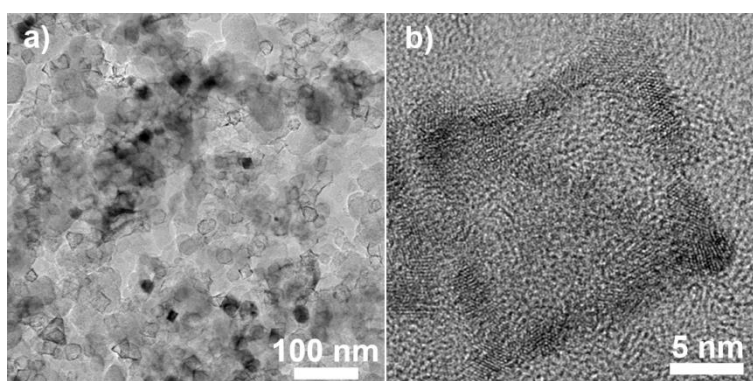

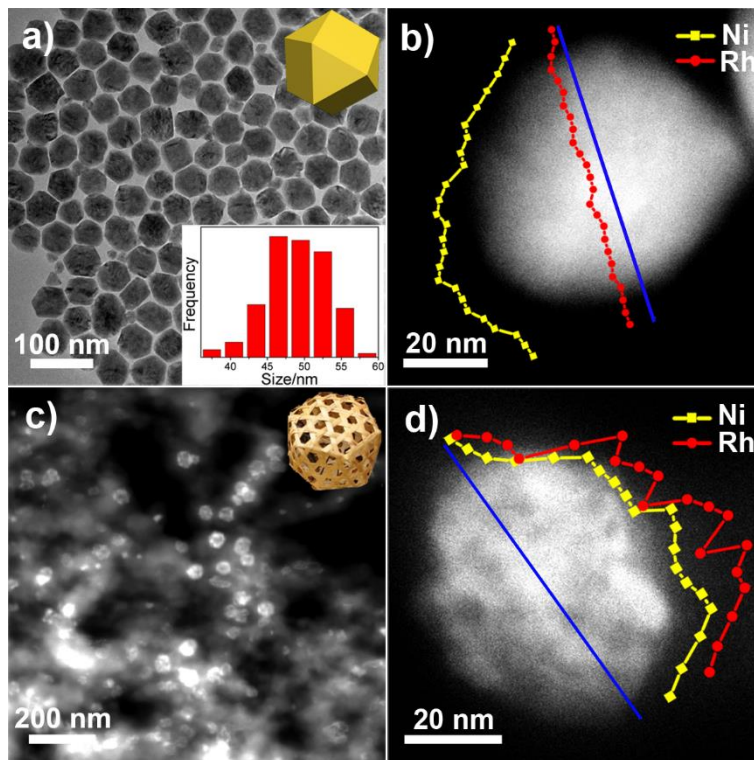***Figure S12.*** TEM image (a), HRTEM image (b) of Rh-Pd-Cu nanopolyhedral frames/C.

Figure S13. TEM image (a) and EDS line scan profiles (b) of Rh-Ni multi-twinned nanocrystals synthesized via the oleylamine solvothermal method. HAADF-STEM image (c) and EDS line scan profiles (d) of Rh-Ni porous nanoframes/C via HCl/O$_2$ etching. Inset in panel (a) is the size distribution histogram of Rh-Ni multi-twinned nanocrystals.
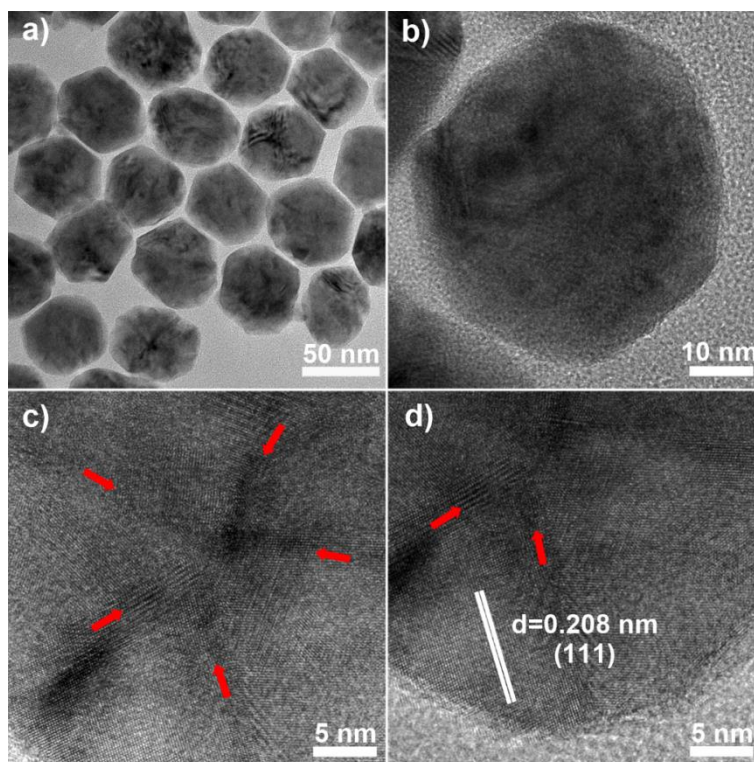
Figure S14. (a) TEM image, (b) magnified TEM image, (c) and (d) HRTEM images of Rh-Ni nanopolyhedrons. The red arrows in panel (c) and (d) indicate the locations of the (111) grain boundaries in a single nanoparticle, so the as-prepared Rh-Ni nanopolyhedrons are multi-twinned nanocrystals.
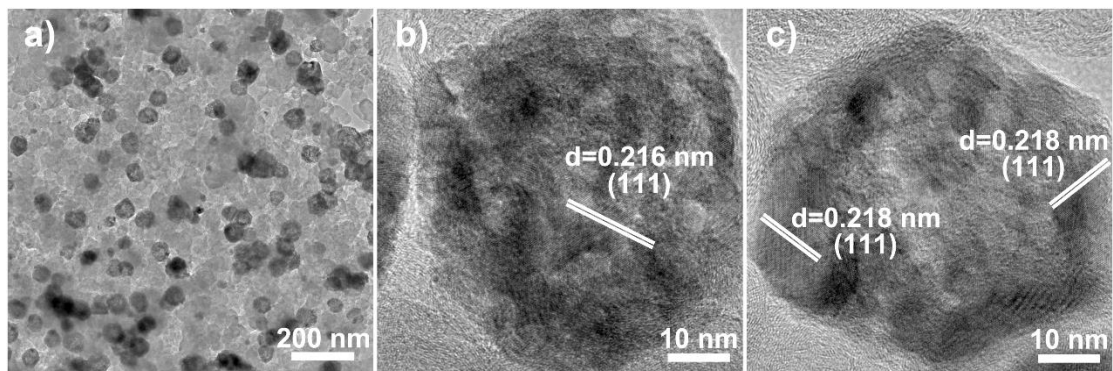

Figure S15. (a) TEM image, (b) and (c) HRTEM images of Rh-Ni nanopolyhedrons/C of Rh-Ni nanopolyhedrons/C after treated in acetic acid.
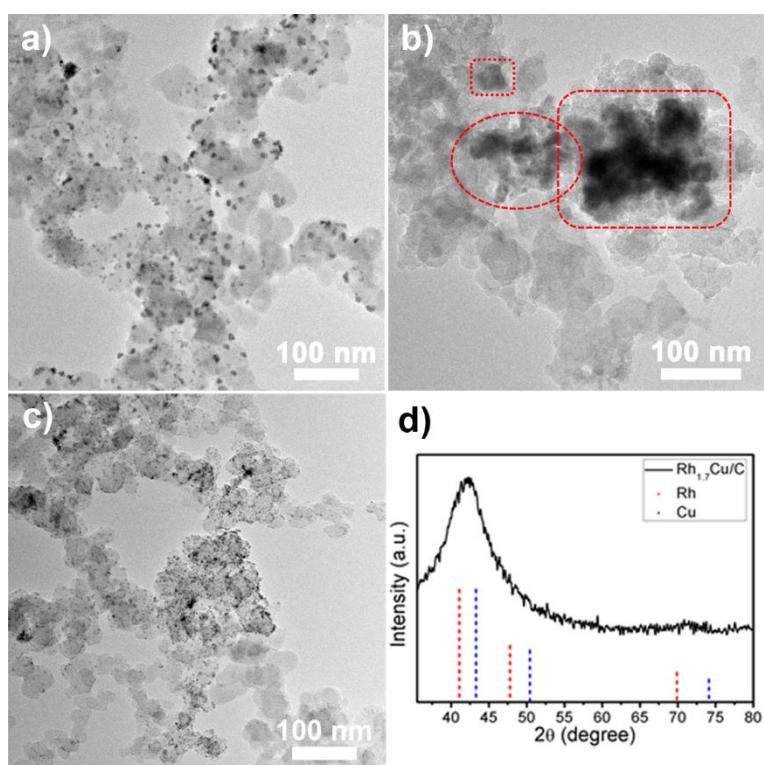

Figure S16. TEM images of (a) Rh/C (the loaded content of Rh was 9.4 wt%), (b) Cu/C (the loaded content of Cu was 15.1 wt%), (c) $Rh_{1.7}Cu/C$ (the loaded content of Rh was 13.3 wt%) synthesized via $NaBH_4$ reduction, and (d) XRD pattern of $Rh_{1.7}Cu/C$.
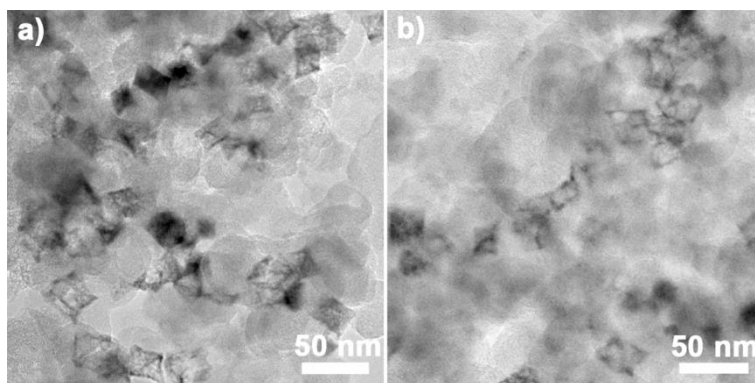
Figure S17. TEM images of Rh-Cu nanooctahedral frames/C after the catalytic reactions of hydrazine decomposition for the second cycle (a) and the fourth cycle (b).

Ref. S1 S. K. Singh, X. B. Zhang and Q. Xu, *J. Am. Chem. Soc.*, 2009, **131**, 9894.

Ref. S2 S. K. Singh and Q. Xu, *J. Am. Chem. Soc.*, 2009, **131**, 18032.

Ref. S3 X. H. Xia, L. Figueroa-Cosme, J. Tao, H. C. Peng, G. D. Niu, Y. M. Zhu and Y. N. Xia, *J. Am. Chem. Soc.*, 2014, **136**, 10878.

Ref. S4 N. Shukla, C. Liu, P. M. Jones and D. Weller, *J. Magn. Magn. Mater.*, 2003, **266**, 178.

Ref. S5 J. F. Moulder, W. F. Stickle, P. E. Sobol and K. D. Bomben, (Eds.: J. Chastain) *Handbook of X-ray Photoelectron Spectroscopy*, Perkin-Elmer Corporation: Minnesota, 1992.